Multi Hydroxyl End Functional Polyethylenes – Synthesis, Bulk and Interfacial Properties of Polymer Surfactants

AUTHOR NAMES

Solomon M. Kimani,[1,2] Richard L.Thompson,[1] Lian R. Hutchings,[1] Nigel Clarke,[1,3] S.M. Reduwan Billah,[1] Victoria García Sakai,[4] Sarah E. Rogers[4]

AUTHOR ADDRESS

1 Durham Centre for Soft Matter, Department of Chemistry, Science Site, Durham, DH1 3LE, UK

2 Present address: Synthomer, Central Road, Templefields, Harlow, Essex, CM20 2BH

3 Present address: School of Physics and Astronomy, Hounslow Building, University of Sheffield, Sheffield, UK

4 STFC ISIS Neutron and Muon Facility, Rutherford Appleton Laboratory, Chilton, Didcot, Oxfordshire, OX11 0QX, UK

AUTHOR EMAIL ADDRESS r.l.thompson@durham.ac.uk

RECEIVED DATE (to be automatically inserted after your manuscript is accepted if required according to the journal that you are submitting your paper to)

TITLE RUNNING HEAD Surface modifying end-functional polyethylenes.

CORRESPONDING AUTHOR FOOTNOTE

* r.l.thompson@durham.ac.uk

tel +44 191 3342139

fax +44 191 334 4737

ABSTRACT

Multi hydroxyl end functional polyethylenes have been prepared with controlled molecular weight, microstructure and functionalization. These materials, designed as interfacially-active blend additives for polar interfaces, are thermally stable up to ~ 250 °C, and to have similar crystallinity and dynamics to their unfunctionalised homopolymers analogues. The polymers segregated strongly to silicon oxide interfaces, with adsorbed layers forming spontaneously at annealed polymer interfaces, having surface excess concentrations approaching 2 R_g, and a maximum areal density of approximately 0.6 adsorbed chains per nm^2. This interfacial activity is achieved almost without detriment to the bulk physical properties of the polymer as evidenced by thermal analysis, quasi-elastic neutron scattering and small-angle neutron scattering (SANS). SANS experiments show little evidence for aggregation of the di-hydroxyl functionalized polymers in blends with PE homopolymers, which is thought to explain why these additives have particularly strong interfacial adsorption, even at relatively high concentrations. A modest level of segregation of the additives to exposed blend surfaces was also seen, particularly when the additive molecular weight was significantly lower than that of the matrix. We attribute this to a combination of the relatively low molecular weight of the additives and the marginally lower surface energy associated with deuterated polymers.

KEYWORDS (Word Style “BG_Keywords”).

Polyethylene, interface modification, dendrimer, adsorption, hydrophobic, semicrystalline

BRIEFS (WORD Style “BH_Briefs”).

Polyethylenes with multiple hydroxyl functional groups can stabilise interfaces without compromising the bulk material properties.

MANUSCRIPT TEXT

Introduction

Polyethylene (PE) has an exceptionally diverse portfolio of applications, from large volume commodity products like packaging to bespoke engineering plastics such as prosthetic joints. This breadth of applications results from the range of material properties that may be accessed by different polymerization routes. The number, length and hierarchical order of branches in different polyethylenes (e.g. LDPE, LLDPE, HDPE etc.) have significant consequences for the melt rheology and solid state properties of these materials even though they are chemically very similar.[1] Despite the wide variety of bulk properties, the surface and interfacial properties tend to be relatively constant. For instance, the liquid surface tensions of linear (67 kg/mol) and branched (7kg/mol) PE are very similar at 35.7 and 34.3 mJ m^{-2} respectively.[2] Polyethylene is chemically quite inert, which for many applications is desirable, but does tend to restrict the options for modifying the surface chemistry. The surface can be oxidised using relatively aggressive chemistry[3] or functionalized by plasma or discharge treatments.[4-6] These methods can be used to increase hydrophilicity, however it is also known that the surfaces are not particularly durable as the high surface energy groups generated by such treatments will tend to migrate into the bulk of the polymer, being replaced by relatively low surface energy PE. A notable limitation of these treatments is that, while they can effectively modify external surfaces of polymers, there is no

scope to modify interactions between PE and solids at buried interfaces, such as are present in filled polymers.

We have in recent years shown that multiple end functional groups, particularly hydrophobic groups on polymer chains, represent a new class of surface modifying additive.[7-16] A key feature of these additives is that the judicious placement of the functional groups on the chain ends can deliver an exceptional degree of surface modification with a very small proportion of hydrophobic component in the polymer. This generic structure is very effective in terms of contributing to surface modification whilst having a relatively small tendency towards aggregation. Although the majority of applications for a blending approach to surface modification would utilize semi crystalline polymers, the vast majority of studies relating to this are focused on amorphous polymers, notably polystyrene.[17-19] One of the few examples of polyethylene surface modification by end functional polymers was reported by Walters *et al*[20] for fluorocarbon functionalised oligomer additives. Recently, however, we have shown that the same approach may also be applied to polyethylene additives above their entanglement molecular weight by using PE with multiple hydrophobic functional groups.[21] The fact that these functionalised polymers were above the entanglement molecular weight is very significant, since this means that the additives themselves have similar bulk properties to the polymers that they might be used to modify. Attempts to reproduce this behavior for hydrophilic polar additives have had limited success. Zhu and Hirt[22] showed that migration to a polypropylene surface is possible for a low molecular weight commercial hydrophilic additive (Irgasurf HL 560), but not for PEG in the same matrix. This is because most hydrophilic additives such as PEG have a higher surface energy than the polyolefin matrix, and therefore would not spontaneously migrate to this surface. The exception reported by Zhu and Hirt had a sufficiently low molecular weight for surface segregation to be entropically favorable,[23] and had a short alkyl chain, which would also favour surface segregation by virtue of having a lower surface energy than polypropylene.

Here, we demonstrate that hydrophilic polar end functional polyethylenes can migrate to and adsorb strongly at polar interfaces of blended films, thereby modifying the interaction between polar materials

and polyethylene. Furthermore, we show that this can be achieved with minimal perturbation to the bulk properties of the matrix polymer. The synthesis of functionalized polyethylenes and influence of the polar functional groups on the thermal stability, crystallinity, mobility, aggregation and interfacial activity of these polymers as additives in blends with homopolymer polyethylene is discussed. We anticipate that additives based on this structure may have considerable utility in the stabilisation of composites and nanocomposites.

Experimental

Synthesis of Multi-hydroxyl end functional PE additives.

We adopt a similar notation to describe these materials as we used in our earlier work on fluorocarbon end functional polyethylenes; namely "*x*OH**P***y*", where *x* is the number of OH hydroxyl groups per functionalized chain end, and **P** denotes the polymer species of nominal mass *y* kg/mol. Hence 2OHdPE22 is a deuterium labeled polyethylene with 2OH groups per chain end and a molecular weight of approximately 22 kg/mol, and PE45 is an unfunctionalised hydrogenous PE homopolymer of 45 kg/mol.

For convenience, the synthesis of multi-hydroxyl functionalized polyethylenes is broken down into two main sections. Firstly, the synthesis of a protected multifunctional end-capping group is shown in scheme 1. These end-capping groups were reacted via their Br group with the living diphenylethylene end of a polybutadiene (PB) chain, and the chain was then saturated with deuterium and deprotected to produce a partially deuterated multi-hydroxyl end-functional polyethylene chain (scheme 2). Using this approach the fraction of deuteration [D]/([H]+[D]) in the resulting polyethylene is approximately 0.4.[21,24] These partially deuterated polyethylenes therefore have sufficient deuterium to provide contrast with hydrogenous polyethylene in nuclear reaction analysis and small-angle neutron scattering experiments, yet also have sufficient protons for their dynamics to be characterized by quasi-elastic neutron scattering. Further details and typical yields for each reaction are included as supporting information. (S.I.1. Synthesis of multi-end functional polyethylenes)

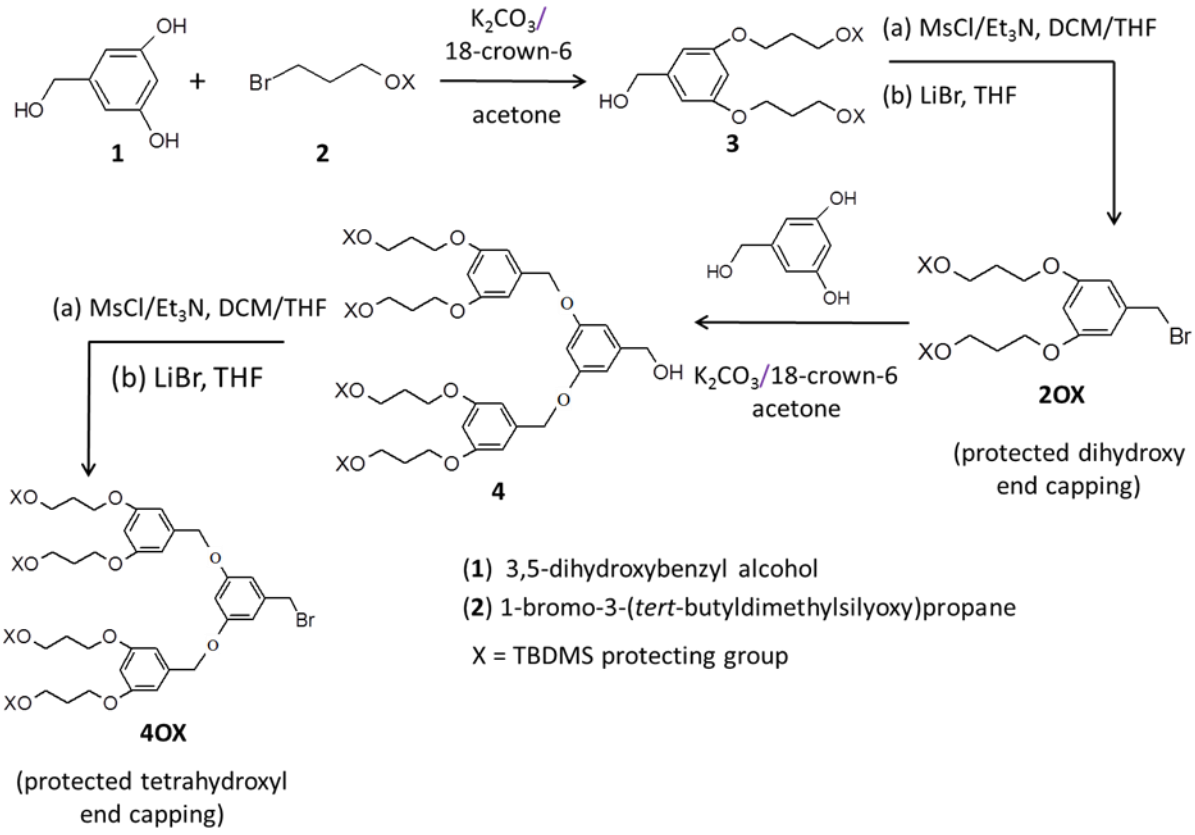

Scheme 1. Synthesis of protected end-capping agents for functionalizing polyethylene.

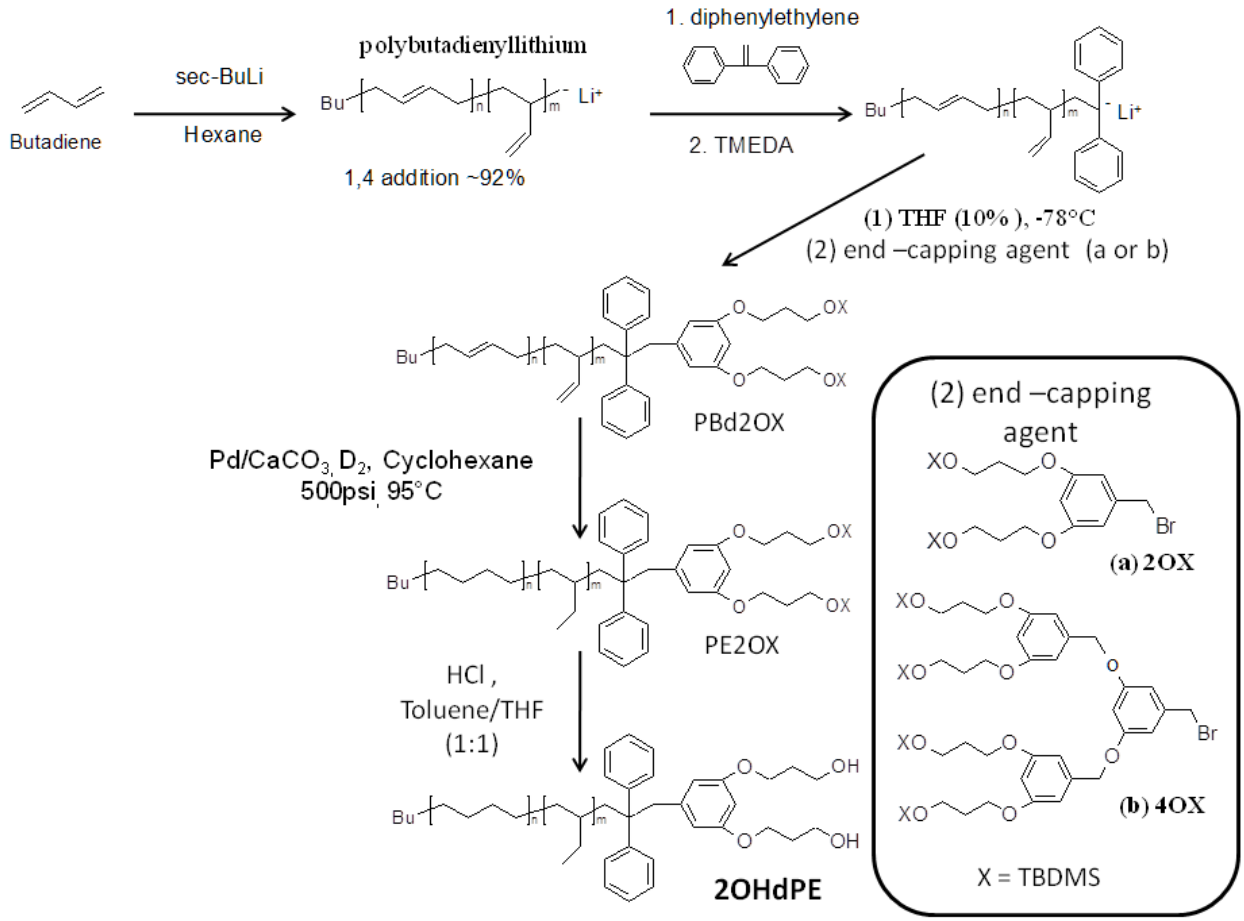

Scheme 2. Synthesis of hydroxyl functionalised polyethylene additives.

Thermal analysis

The thermal stability for the polymers was measured by thermogravimetric analysis (TGA) using a Perkin Elmer Pyris 1 TGA instrument. Analysis was carried out on carefully dried samples (~10 mg) from room temperature up to 350 °C and heating rate of 10 °C per minute. Typical data, showing the extrapolated temperature for the onset of degradation are shown as the supporting information (S.I.2). The melting temperature T_m and enthalpy of melting, ΔH_m was characterized by differential scanning calorimetry (DSC). Heating scans were carried out at 10 °C per minute using a TA instruments Q1000 DSC on samples which had first been raised to well above the melting temperature and then cooled at 40 °C per minute to ensure a consistent thermal history. Samples of approximately 10 mg were weighed

with a precision of 10^{-3} mg in a differential balance to enable quantification of the enthalpy of melting relative to an indium reference standard (T_m = 156.61 °C, ΔH_m = 3.296 kJ mol^{-1})

Quasi elastic neutron scattering (QENS)

QENS experiments were carried out on the IRIS time-of-flight backscattering spectrometer at ISIS Neutron and Muon Facility, Rutherford Appleton Laboratory, UK. QENS is a unique way of probing dynamics of polymer molecules[25-27] and soft matter[28,29] in general, local as well as segmental relaxations as a function of length scale. Furthermore, the mobility of different parts of a polymer molecule can be identified by selective deuteration. IRIS was run using the 002 reflection of a pyrolytic graphite analyser which affords an energy resolution of 17.5 μeV, and a standard measurement energy window of ± 0.5 meV. This setting allows us to probe motions at timescales ranging from 2 ps to 200 ps, and based on the angular coverage of the detectors, length scales ranging from 4 Å to 16 Å. QENS measurements were run as a function of temperature on pure samples of the multi-end functionalized polyethylenes. Polymer samples were melt pressed at 120 °C into 65 mm × 30 mm rectangular sheets of an average thickness of 0.15 mm in order to minimize multiple scattering effects. The films were rolled into annular aluminium cans to ensure full detector coverage.

Small angle neutron scattering (SANS)

The extent of aggregation of end functional polyethylenes in blends with polyethylene homopolymers was determined by small-angle neutron scattering. SANS experiments were carried out using the SANS2D diffractometer on TS2 at ISIS Neutron and Muon Facility, Rutherford Appleton Laboratory, UK. Collimation was fixed at 6 m to the sample and the detector was fixed at 6 m from the sample, with vertical and horizontal detector offsets of 170 mm and 100 mm respectively. An 8 mm diameter beam of neutrons of wavelength 1.75-16.25 Å were scattered by samples of 30 mm x 10 mm x 1 mm polyethylene blends, melted into Quartz cuvettes, and thermostatted to 120 °C to ensure that they were

molten during data acquisition. Data were obtained over a scattering vector range $0.0035 < Q / Å^{-1} < 0.5$ in a single measurement.

Nuclear reaction analysis (NRA)

NRA experiments were carried out at Durham University using a National Electrostatics Corporation 5SDH Pelletron accelerator. Thin film samples of PE blends were prepared by co-dissolving and spin-coating as described previously.[21] The films appeared smooth to the naked eye, but AFM topography scans (included as supporting information S.I.3) clearly revealed the crystalline structure, and the r.m.s. roughness was of the order 5-10 nm, as opposed to <1 nm that would be expected for amorphous spin-cast films of this thickness. A 0.7 MeV $^{3}He^{+}$ beam was brought onto the samples of the grazing incidence angle of 80° to the sample normal, and backscattered reaction products were analysed at 170° to the incident beam in Cornell geometry. Due to the relatively low levels of deuteration in the partially-labelled blended samples, it was necessary to make 2-5 measurements on separate spots of each sample in order to obtain good statistical quality of data without artifacts arising due to beam damage. The total beam charge delivered to any one spot was restricted to 3 μC. The nuclear reaction analysis technique[30] application of ion beam analysis to polymer materials has been reviewed elsewhere.[31,32]

Results

Synthesis and Characterization of Multi-Hydroxyl End Functional Polyethylenes

Scheme 2 shows the chemical structure of the multi hydroxyl end functionalised polyethylenes. It should be noted that although these polyethylenes were produced by hydrogenation of polybutadiene, the route to making these materials differs significantly from that used for our earlier work on mult-hydroxyl end functionalized polybutadienes.[15] The reason for this is that the previously reported functionalized polybutadienes were end-functionalized by a click reaction and the end groups were not stable with respect to catalytic hydrogenation or deuteration. In the present work we therefore used an approach to end capping polybutadiene, followed by saturation with hydrogen or deuterium, which we

have previously found to be a robust method for the production of analogous fluorocarbon end functionalised polyethylenes.[21]

Table 1. Summary of SEC, NMR and thermal analysis data for polybutadiene precursor polymers and their saturated, end-capped PE analogues.*

Polymer Sample	M_n[a] / kg mol^{-1}	M_w[a] / kg mol^{-1}	% 1,4[b]	% end capping	% saturation	T_m / °C	ΔH_m J/g[c]	T_d / °C
2OHdPE6	6,100	6,400	92.7	89	98	103.9	102.7	245
2OHdPE11	11,300	11,800	92.8	90	97	106.3	116.1	245
2OHdPE18	18,300	19,200	92.9	83	98	107.3	103.9	245
2OHdPE22	22,500	23,300	93.1	85	99	106.9	83.9	246
4OHdPE8	7,500	7,900	93.0	97	98	104.1	98.4	267
4OHdPE11	10,900	11,703	92.9	92	98	107.8	109.8	262
4OHdPE18	17,000	17,900	92.6	85	97.5	109.1	112.8	283
4OHdPE30	30,200	32,500	92.3	87	98	105.1	79.4	258
hPE (high 1,4)	44,100	45,300	93.5	N/A	99.5	113.4	97.9	246
hPE20:80 (low 1,4)	34,300	33,000	80.0	N/A	99.5	50.0	47.5	250

[a]% 1,4-microstructure obtained from the NMR results (^{1}H C_6D_6)

[b] Molecular weight determined using triple detection SEC

* Number average (M_n) and weight average (M_w) molecular weights were determined by SEC in THF of the polybutadiene precursor. The fraction of 1,4 PB enchainment and % end-capping were determined by ^{1}H NMR in C_6D_6. The percentage end-capping was determined by high temperature NMR in d-xylene. The melting temperature, T_m, enthalpy of melting, ΔH_m and decomposition temperature T_d were determined by DSC and TGA.

The data summarized in table 1 show that the synthetic methodology is appropriate for the synthesis of end functionalized polyethylenes with very high degree of control over molecular weight, dispersity, microstructure and a high degree of end-capping.

The melting temperature, T_m, and enthalpy of melting values, ΔH_m were found to be ~110 °C and ~100 J/g, for most PEs, with no strong dependence on molecular weight or functionality. The largest single factor governing these values is the nature of PB enchainment prior to saturation, which dictates the final proportion of ethyl pendant groups on each PE chain. This is exemplified by the hPE20:80 sample, which was deliberately prepared to contain a greater proportion of 1,2-enchainment than would be achieved by carrying out the polymerization in pure hexane. The modification to the microstructure was achieved by the inclusion of a very small amount of THF (0.3 mol THF per mol of sec-BuLi initiator) to the reaction mixture. This relatively small perturbation to the in-chain microstructure was sufficient to reduce the melting enthalpy by a factor of 2, and reduce the melting temperature by approximately 60 °C.

Dynamics in the solid state

Quasi elastic neutron scattering probes the dynamics of atoms in the polymer sample by measuring the exchange in momentum and energy between atoms and the neutrons. Due to the strong interaction of the neutron with hydrogen atoms (incoherent scattering cross-section ~80 barns for ^{1}H, 2 barns for ^{2}H and zero for C and O), the majority of the signal comes from the mobility of the protons. An array of detectors surrounding the sample records the angle and energy dependent intensity of scattered neutrons $S(Q,E)$ defined by the double differential scattering cross section, $\partial^2\Sigma/\partial E\partial\Omega$. Figure 1 shows typical data for the dependence of the QENS signal on scattering vector Q (defined as 2π/lengthscale) and functionalisation. Zero energy transfer indicates elastic scattering events (convolved by the instrumental resolution), i.e any motion which is too slow to be captured, whereas the broadening is the QENS signal arising from protons moving in the timescale of the spectrometer. The data show a strong dependence on Q, indicating that within the accessible time window the motion of protons in the sample is clearly distinguishable over different length scales. It is also notable that for all the values of Q, the hPE homopolymer and the 4OHdPE11 multi-end functional polymer have very similar dynamics. This

indicates that the dynamics of the multi hydroxyl functionalized polyethylenes are very similar to their unfunctionalised counterparts.

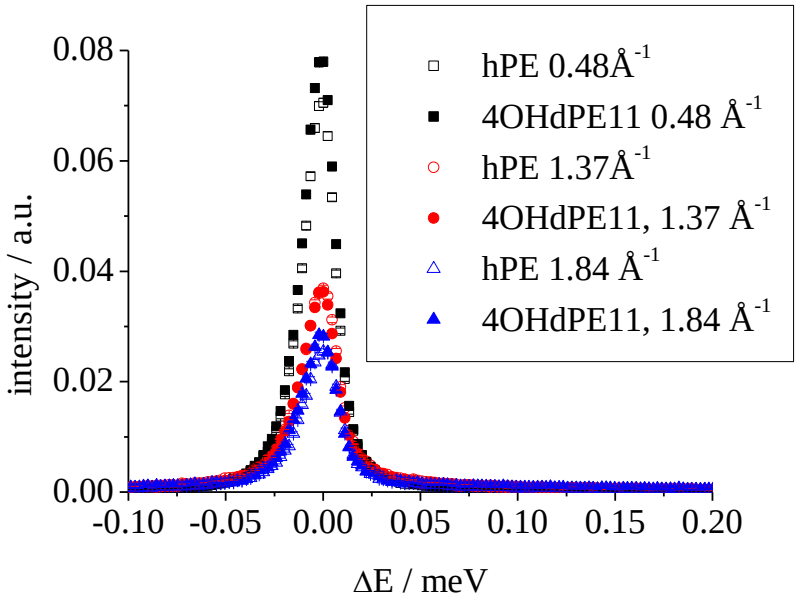

Figure 1. Dynamic incoherent structure factor, $S(Q,E)$ for 4OHdPE11 and hPE at 75 °C.

The data were normalized to incoming beam intensity and detector efficiency corrections applied based on a vanadium standard measurement, using the *MODES* v3 software available at ISIS[33]. Data analysis was performed in the time domain, by Fourier transforming the measured intensity $S(Q,\omega)$ to obtain the intermediate scattering function, $I(Q,t)$ using the *DAVE* analysis package made available by NIST Center for Neutron Research, NCNR.[34] The characteristic relaxation time, τ, as a function of temperature and scattering vector was obtained by fitting a Kohlrausch Williams Watts (KWW) stretched exponential function to the intermediate scattering function,

$$I(Q,t) = A\exp\left(-\left(\frac{t}{\tau}\right)^{\beta}\right) + B \qquad (1)$$

where A and B correspond to the mobile and immobile fractions of protons within the time scale of the QENS experiment and β is the stretching exponent, which for most polymers is around 0.4-0.6.

Small-angle scattering

Figure 2 shows typical small neutron scattering data and fits in which the aggregation of end functionalised polyethylenes into micelles can be quantitatively simulated using the random phase approximation.[35] In the simplest case, assuming no aggregation, the effective aggregation number of each chain, N_{agg}, would be exactly 1, and the structure factor for the polymer chain $P(Q)$ is simply the Debye scattering function,

$$P(Q) = \left(\frac{2}{u^2}\right)\left[\exp(-u) - 1 + u\right] \qquad (2)$$

where $u = (QR_g)^2$ and R_g is the radius of gyration of the PE, given by

$$R_g / nm = \left(\frac{0.0121 M_w}{6}\right)^{1/2} \qquad (3)$$

In order to avoid over-parameterization of the fits to the small angle scattering data, the R_g values were fixed at the unperturbed dimensions obtained from equation 3. If the multiple-hydroxyl groups on the polymers on the chain ends caused aggregation, then we would expect that these aggregates would take the form of an inverse micelle with a small hydroxyl-rich core surrounded by a corona of polymer chains. It is relatively straightforward to modify the structure factor to allow for inverse micelles by representing them as star shaped polymers, where the number of arms is equal to N_{agg}.[7] For much larger aggregates, as would be expected in the event of phase separation, the scattering intensity at low Q would be dominated by the interface between aggregates in the additive-rich phase and the surrounding matrix-rich phase. The data in figure 2, which are typical of all of the data obtained for blends containing 2OHdPE*y*, show very little evidence for aggregation; i.e. N_{agg} is little more than 1. Here, we have presented the data and fits for the highest concentrations additives, which have the highest density of functional groups that we were able to study. The impact of the N_{agg} on the scattering data is shown in some quantitative simulations as supporting information in S.I.4.

Unfortunately we were unable to melt any of the 4OHdPE*y* samples into the cuvettes used for these experiments before significant degradation became evident through the browning of the polymers. The

fact that these blends did not flow as readily as the 2OHdPE*y* blends could be consistent with a higher viscosity, suggesting that aggregation may in fact occur for the polymers bearing the larger functional groups.

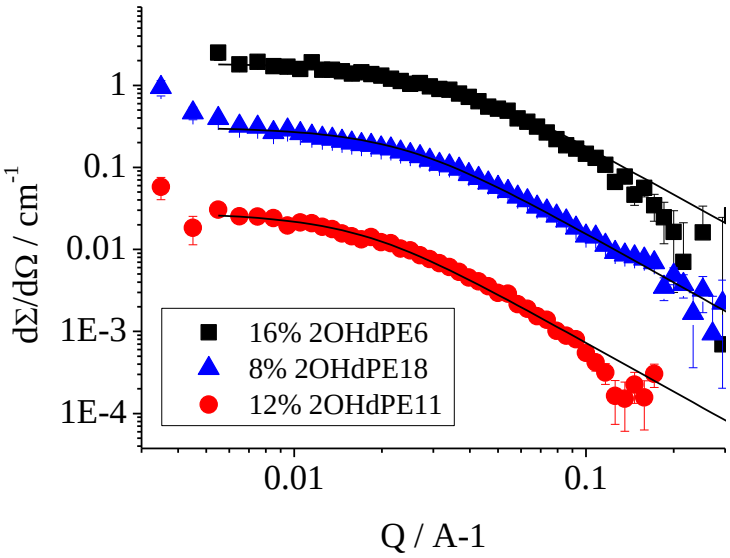

Figure 2. SANS data and fits for 3 blends of 2OHdPEy in hPE. Data are offset by successive factors of 10 below 16% 2OHdPE6 for clarity. The solid curves are the fits obtained with N_{agg} values of 1.22, 1.59 and 1.67 for 16% 2OHdPE6, 12% 2OHdPE11 and 8% 2OHdPE18 respectively.

Nuclear Reaction Analysis

The extent to which the multi-hydroxyl end functional polymers could adsorb to and modify the interface of a model polar surface was characterized by nuclear reaction analysis. The silicon wafers had a native oxide layer of approximately 3 nm silicon oxide, and are therefore representative of the surface of the silica nanoparticles and fibers.[36] Typical data for these experiments are shown in figures 3 and 4. The data detected at lowest energy (in this case ~channel 1309) corresponds to nuclear reactions occurring close to the sample surface, and events occurring deeper within the film are detected at higher energy of backscattered proton.[30] The D(^{3}He,p)α nuclear reaction cross section varies smoothly over the energy range for which data were obtained, but is most sensitive to deuterium near the sample surface. The peak in the data seen around channels 1320-1330 therefore corresponds to a considerable accumulation of the deuterated additive at a buried interface. Data were analysed using the Surrey

University Datafurnace[37] software, which was used to simulate the NRA spectra for a simple slab like concentration profile and fit these spectra to the experimental data by varying the composition and thickness of the layers. A typical concentration versus depth profile is shown in the inset. The fits to the data are the smooth curves shown in figures 3 and 4. In some cases a smaller peak at the low channel end of the spectrum was also seen, which can only be due to the small surface excess at the exposed surface of the film.

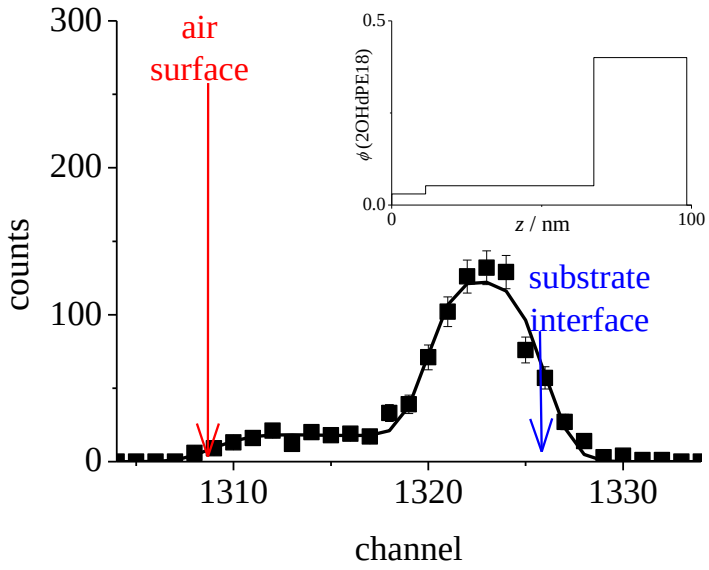

Figure 3. Nuclear reaction analysis data and fit for 16% 2OHdPE18 in hPE. The solid curve is the fit to the experimental data corresponding to the concentration profile in the inset.

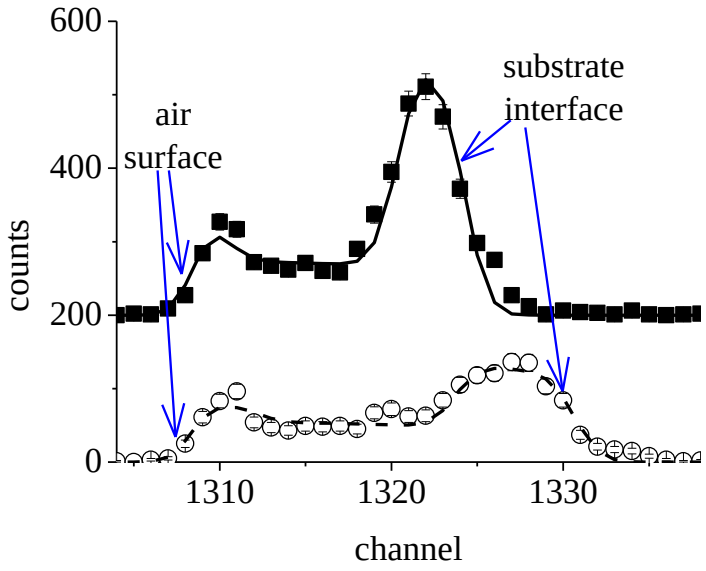

Figure 4. Nuclear reaction analysis data and fits for 16% 4OHdPE8 (open circles) and 2OHdPE6 (solid squares, offset by 200 counts for clarity). The curves are the fits to the experimental data.

Discussion

Materials

The purpose of our present work is to determine the influences of molecular weight and functionality on the bulk and interfacial properties of multi-hydroxyl end functional polyethylenes and blends of these materials with unfunctionalized polyethylene. Characterization of the polymers (shown in table 1) demonstrates that the methodology is appropriate to prepare gram quantities of very well defined polyethylenes with a high degree of precisely controlled functionality.

It is worth noting that for these polymers, the end functional groups are a very small fraction of the total volume of the polymer chains. We calculate that the contribution of the 2OH and 4OH functional groups (including the diphenylethylene groups) to the polymer chain volume is approximately 400 $Å^3$ and 700 $Å^3$ respectively, and is dominated by the aromatic moieties present.[38] By comparison, even the lowest molecular weight polymer prepared, 2OHdPE6 has a volume of approximately 11000 $Å^3$ per polymer chain.

The single greatest factor affecting the bulk physical properties is the variation in chain microstructure, rather than the functionalization. Assuming as a first approximation that T_m decreases linearly with increasing 1,2 content in the PB precursor, we obtain a value of nearly 5 °C reduction in T_m per percent of 1,2 enchainment. Although this is a crude approximation, it is reassuring to note that this figure would suggest a melting temperature of approximately 140 °C for perfectly linear PE in the absence of any 1,2 enchainment. This is consistent with the range of melting temperatures reported for linear high density polyethylenes,[39] and is consistent with the observation in earlier QENS experiments that end group effects in unmodified PE are usually only apparent for oligomers.[40] Although the correlation between T_m and microstructure is not clear within the uncertainty of these parameters, it is worth noting that when the microstructure is consistent to within 1%, a variation in T_m of approximately 5 °C might be expected. Our thermal analysis results are similar to our earlier results for fluorocarbon end functionalized polyethylenes,[21] and ΔH_m of ~100 Jkg^{-1} corresponds to approximately 40% crystallinity. The similarity between T_m values, irrespective of functionalization is a very desirable feature of the multi-hydroxyl functionalized polymers, since it indicates that they could be used as additives over a wide range of concentration without significant detriment to the bulk material properties of their blends.

All of the polymers synthesised exhibited a very similar degree of thermal stability irrespective of microstructure. This is important for future applications of these materials since it clearly shows that there is a window of well over 100 °C between the melting point and the point at which the materials become unstable in which samples can be processed or allowed to reach equilibrium.

Solid State Dynamics of Pure Polyethylenes and Additives

Fitting the *I(Q,t)* data using equation 1 quantified the dynamics of the materials and provided some insight into the impact of incorporating end-functional groups into polymer chains that are expected to be too bulky be incorporated into crystalline domains. In most of our measurements, β values were

found to be 0.6 ± 0.1, and subsequently this parameter was fixed at 0.6 throughout. Typical results for these fits are shown in figure 5, and a rigorous analysis and interpretation of the QENS data is included as supporting information in S.I.5. For the purposes of the present discussion, the key observations are that our results for the multi-hydroxyl end functionalized polymers are consistent with those obtained by other groups for unfunctionalised homopolymers, [40-42] and are dominated by the localized motion of the amorphous domains.

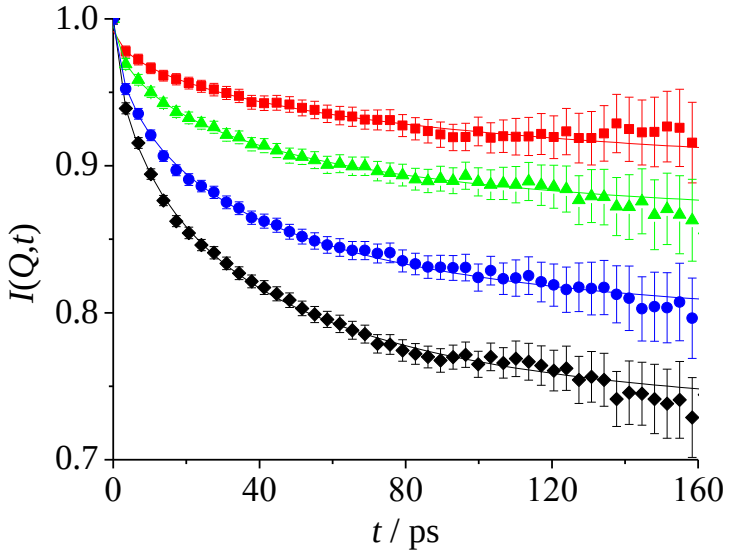

Figure 5. Stretched exponential fits to derived $I(Q,t)$ data for 4OHdPE11 as a function of temperature: 25 °C (red squares), 50 °C (green triangles), 75 °C (blue circles) and 100 °C (black diamonds). Results are for $Q = 0.48$ Å^{-1}.

Aggregation of multihydroxyl end-functional PEs in blends

Aggregation (e.g. micellisation) of surface or interface modifying polymers in molten blends is normally an undesirable quality, as this phenomenon is likely to hinder the migration of an additive to an interface. Furthermore, aggregation of polar end functional polymers is challenging to predict *a-priori* as the polar groups have anisotropic interactions, and have the further complication of being attached to a polymer chain, and the 'solvent' in this case is also polymeric; a factor generally well handled by solubility parameter methods.[38] The aggregation behavior several 2OHdPEy materials in

blends with hPE was therefore followed by small-angle neutron scattering. Deuterium labeling is known to give rise to a small positive Flory–Huggins interaction parameter, χ_{hd}, which was established by Nicholson *et al*.[43] for similarly labeled PE homopolymers to be

$$\chi = 1.14 \times 10^{-3} f^2 \tag{4}$$

where f is the fractional deuteration previously established for dPEs made in an identical way to be approximately 0.4. According to Flory Huggins theory,[44] the criterion for phase separation due to incompatibility of the polymer chains is a negative value for the second derivative of the free energy of mixing,

$$\frac{\partial^2 \Delta G_{mix}}{\partial \phi^2} = \frac{1}{N_1 v_1 \phi} + \frac{1}{N_2 v_2 (1-\phi)} - \frac{2\chi}{v_e} < 0 \tag{5}$$

where N_i and v_i are the degree of polymerization and repeat unit volume of the i^{th} component and v_e is a reference volume, often given as the geometric mean of the repeat unit volumes. Phase separation would be most probable for the highest molecular weight polymer pair (28 kg/mol dPE, 45 kg/mol hPE, where N_1 and N_2 are highest) and the highest volume fraction of additive (0.16). We estimate that spontaneous phase separation would only occur for $\chi > 0.007$. In fact the influence of isotopic substitution on χ is more than an order of magnitude smaller than this ($\chi \sim 0.0002$) and had almost no discernible effect on the calculated differential scattering cross section when compared to $\chi = 0$ (see information S.I.6). Although one should be wary of using Flory Huggins theory to predict phase boundaries, the fact that the interaction parameter is more than an order of magnitude too weak to indicate that phase separation would occur for the most incompatible blend demonstrates that isotopic substitution is unlikely to have any discernible impact on aggregation measured in these blends.

The results for N_{agg} as a function of composition and additive molecular weight presented in figure 6 demonstrate that aggregation is not very significant for these additives in blends with a homopolymer. In fitting the small angle neutron scattering data, the radii of gyration were fixed at the calculated

unperturbed dimensions and excellent fits to the data were found with the small aggregation numbers of 1 to 3. For such small aggregates, little stretching of the chains away from the inverse micelle core would be expected for low values of N_{agg}.[45] The observation of aggregation numbers slightly greater than one does suggest that there is some attraction between the polar end functional groups when dispersed in a non-polar PE matrix, possibly resulting in dimer formation. Nevertheless, there was no evidence for large aggregates as we have seen previously for 4×C_8F_{17}-fluorocarbon end functionalised polystyrenes.[7]

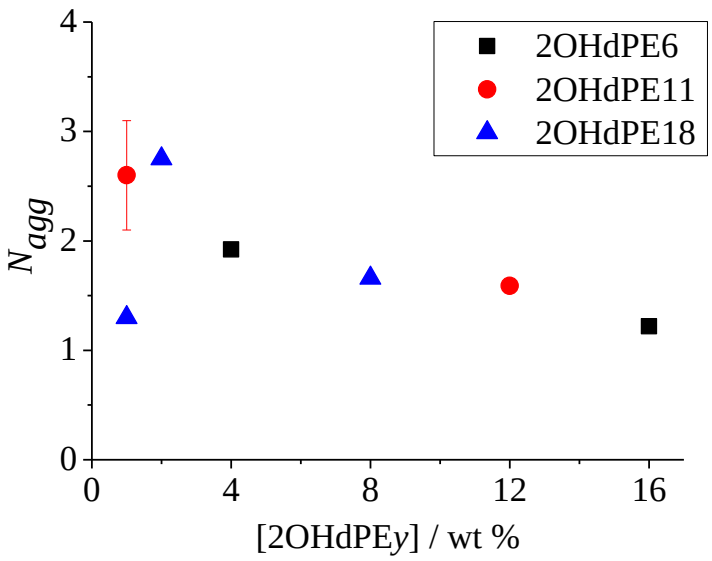

Figure 6. Aggregation number of multi-hydroxyl end functional polyethylenes as a function of molecular weight and concentration.

The scatter in the observed values for the aggregation number is largest for the lower concentrations of additive, which arises from the fact that these partially labeled polymers are moderately weakly scattering. Some further uncertainty is likely to arise from small variations in the effective sample volume present in the beam. In some samples, after heating to above the melting point, it was noted that small bubbles had formed in the path of the beam, effectively reducing the of volume of scattering material. We therefore expect some of the measured aggregation numbers to be slightly lower than the

true values, but not to the extent that the presence of large aggregates could be justified. Interestingly, there was no significant trend in either molecular weight or concentration on the aggregation of these materials. The 2OH end functional PEs have a very similar degree of endcapping (80 to 90%), so the number of end functional groups per unit volume will scale inversely with M_n. It follows that the 16% 2OHdPE6 sample has approximately 50 times the concentration of functional groups as the 1% 2OHdPE18 sample. Since both materials have N_{agg} values of close to one, it can be concluded that the 2OH groups have little effect on aggregation of end functional polyethylenes, and that our blends exist as a single phase in the melt.

Surface and Interfacial Activity of xOHdPEy in blended films

Having established that the *x*OHdPE*y* additives have very similar bulk properties to their unfunctionalized counterparts and exhibit, we now turn our attention to their surface and interfacial properties. In all blended films there was a substantial accumulation of the multi-hydroxyl functionalized PE additive at the film – silicon interface, indicated by the major peaks in proton yield (counts) versus energy (channel) shown in figures 3 and 4. Surprisingly, there was also in many cases a smaller peak in the spectra around channel 1310, corresponding to the film surface. In other words, the nuclear reaction analysis experiments are unambiguously indicating some accumulation of the polar end functional additive at the film surface. This unexpected feature suggests the possibility to use these additives to deliver polar functionality to film surfaces. The reason for this effect is not completely clear, however we note that surface enrichment is most evident for the lowest molecular weight additives, regardless of their functionalization. This suggests that segregation to the air surface of blended films may be driven by the difference in molecular weight, which has previously been established by Hariharan *et al* in isotopic blends.[23] In the case of the materials in this study, both their relatively low molecular weight and their labeling with deuterium could be expected to contribute to the modest levels surface activity observed. Other explanations seem less likely for our blended films: oscillating concentration profiles are often generated at intermediate stages surface or interfacially

directed spinodal decomposition.[46,47] However, given the likely variation in diffusion coefficients between different additives it would seem improbable that each would so often arrive at the same final state after the same period of annealing. Partial dewetting of the film above a wetting layer of *x*OHdPE*y*, could also yield such data as the ion beam would detect the exposed interfacial wetting layer as being at the sample surface. This phenomenon was shown by Stamm *et al* for strongly adsorbing end-functional polystyrenes, where annealed films would dewet, but could leave a monolayer of adsorbed end functional polymer on the substrate surface.[48] However, our AFM analysis of the film surfaces reveals only a modest variation in film height, with r.m.s. surface roughness of the order of 10 nm, which is not consistent with dewetting of a film of ~100 nm total thickness. Furthermore, our AFM measurements showed no evidence of gaps or pinholes of sufficient depth for the substrate interface to be exposed. The well resolved peak in the raw data corresponding to the excess of *x*OHdPE*y* at a buried interface also provides compelling evidence for the integrity of the polymer film over macroscopic areas. If there were significant variations in effective film thickness overlaying the interfacial excess layer due to dewetting or other defects, then this major peak would be smeared out and the region of the spectrum corresponding to the substrate interface would be much more diffuse than the air surface of the film. The irradiated area of the sample by the ion beam is defined by the 2.4 mm diameter beam spot, which is projected as an ellipse at grazing incidence. After repetition over multiple spots to minimize beam damage, the irradiated area is of the order of 1 cm^2, and it is clear that the apparent depth of the substrate interface is well defined.

The most convenient measure of the extent of interfacial activity is the surface (or interfacial excess), defined here as

$$z^* = \int_0^{z_b} (\phi(z) - \phi_b) dz \qquad (6)$$

where $\phi(z)$ is the depth dependent volume fraction and ϕ_b is the volume fraction of additive in the bulk of the film and z_b is the depth at which the volume fraction of additive reaches a minimum. Results for the derived values of interfacial excess as a function of bulk additive concentration and additive chain

molecular weight, *y*, are shown in figures 7 and 8 for 2OHdPE*y* and 4OHdPE*y* respectively. There is a clear increase in z^* as a function of ϕ_b for every *x*OHdPE*y*, which is in keeping with our previous observations for other end-functional additives.[7,8,21] However, in contrast to many of our other studies, we observe that z^* typically grows almost linearly with increasing ϕ_b up to a maximum value at ϕ_b = 0.16. In earlier studies where there was also evidence of significant micellisation, z^* was seen to increase sharply with initial increasing concentration, before reaching a plateau at some value, which was consistent with the onset of aggregation. In our present work there is very little evidence for aggregation of 2OHdPE*y*, so it is not perhaps surprising that the behavior is different. In fact, when the total amount of 2OHdPE*y* present in the film is taken into account, the observed behavior corresponds to a very high proportion of the additive accumulating at the film-substrate interface, leaving a relatively small proportion of the additive in the bulk.

Interestingly, the addition of two further OH groups per additive polymer chain does little to enhance interfacial segregation, and may even decrease the maximum values of z^* obtained. Generally these data show little increase in z^* when increasing ϕ_b from 0.08 to 0.16, in contrast to the near linear increase seen for 2OHdPE*y*. We speculate that this is indicative of aggregation of the 4OHdPE*y* additive, which could reduce the rate at which this additive can diffuse to the substrate interface. By analogy to surfactant systems, the point at which aggregation occurs demarks the concentration at which further increases to the additive concentration have little effect on the activity, and therefore little influence on the equilibrium interfacial concentration of additive. This hypothesis is also consistent with the greater viscosity of the materials that was apparent from our unsuccessful attempts to melt these blends into quartz cuvettes for the SANS experiments.

It is noticeable that for all of the *x*OHdPE*y* materials, over a broad range of concentration, there appears to be a maximum in the measured surface excess in the middle of the molecular weight range that was tested. At low molecular weights, the increase in z^* with increasing M_w is largely due to the fact that z^* measures the total amount of adsorbed polymer, and not the number of chains per unit area.

At higher molecular weights, the trend reverses as adsorption of high molecular weight chains is opposed by the conformational entropy loss associated with surface confinement. Our previous work on fluorocarbon end functional polyethylenes demonstrated that crystallization of the blended films below T_m had little effect on the measured surface excess, and therefore we were able to make some comparison between our experimental data and predictions from SCFT models in which the degree of polymerization of the functional polymer and matrix are defined and the affinity of the functional group for an interface may be varied.[49] The observed maximum in surface excess is qualitatively reproduced with approximate agreement between surface excess values by SCFT models when the attraction of the functional groups for the substrate interface is approximately 6 k_BT (see supporting information S.I.6).

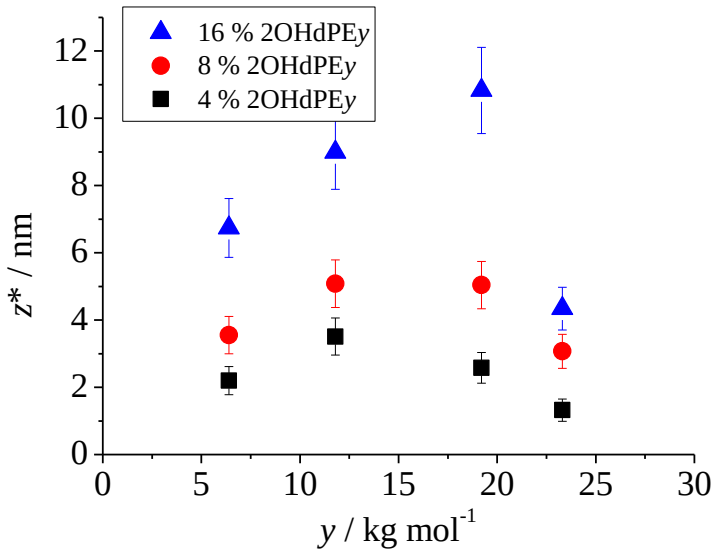

Figure 7. Interfacial excess as a function of 2OHdPE*y* molecular weight and concentration.

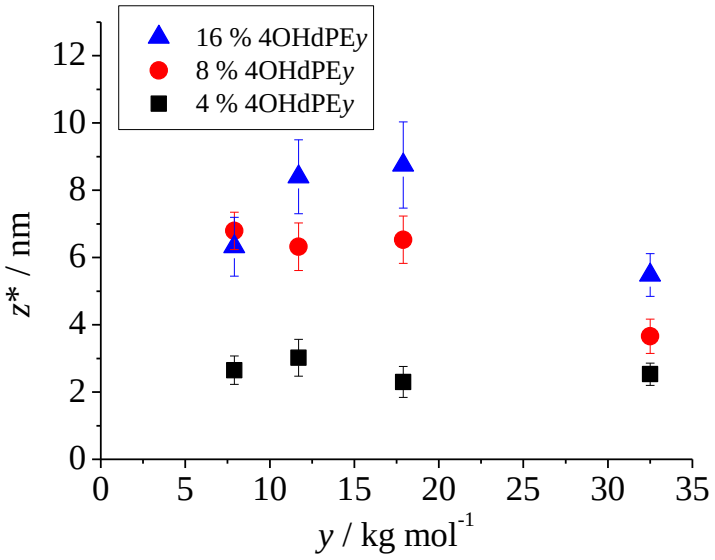

Figure 8. Interfacial excess as a function of 4OHdPE*y* molecular weight and concentration.

It is noticeable that for all of the *x*OHdPE*y* materials, over a broad range of concentration, there appears to be a maximum in the measured surface excess in the middle of the molecular weight range that was tested. At low molecular weights, the increase in z^* with increasing M_w is largely due to the fact that z^* measures the total amount of adsorbed polymer, and not the number of chains per unit area. At higher molecular weights, the trend reverses as adsorption of high molecular weight chains is opposed by the conformational entropy loss associated with surface confinement. Our previous work on fluorocarbon end functional polyethylenes demonstrated that crystallization of the blended films below T_m had little effect on the measured surface excess, and therefore we were able to make some comparison between our experimental data and predictions from SCFT models in which the degree of polymerization of the functional polymer and matrix are defined and the affinity of the functional group for an interface may be varied.[49] The observed maximum in surface excess is qualitatively reproduced with approximate agreement between surface excess values by SCFT models when the attraction of the functional groups for the substrate interface is approximately 6 k_BT (see supporting information S.I.7). If the surface excess data are normalized with respect to the polymer molecular volume, then the

interfacial excess can be expressed in terms of adsorbed chains per unit area, Γ. In this format, (figure 9) commonly used in surfactant science literature, the influence of molecular volume is seen to dominate the behavior and Γ decreases monotonically with increasing molecular weight. Finally, it can be seen that the maximum areal density achieved is approximately 0.6 chains of 2OHdPE6 per nm^2. This value appears to be limited by the PE chain dimensions rather than the estimated size of the functional group, which we estimate could pack at more than twice this density at saturation.

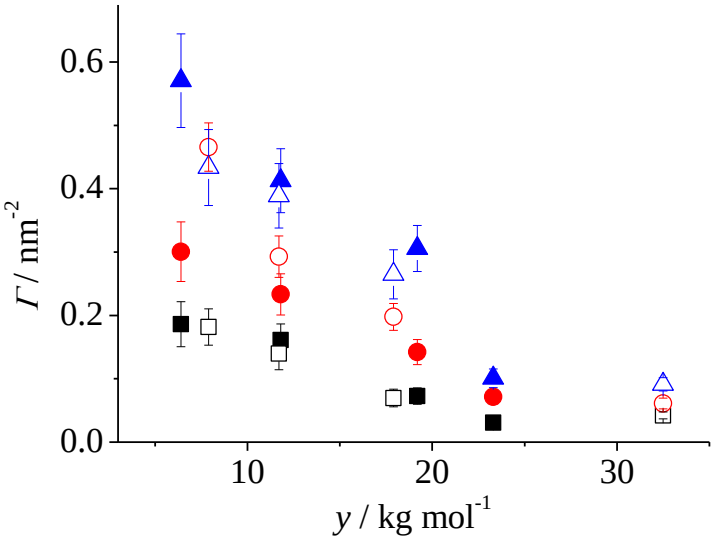

Figure 9. Comparison of interfacial excess behavior for 2OHdPEy (solid symbols) and 4OHdPEy (open symbols) expressed as adsorbed chains per nm^2.

Conclusions

Two series of interfacially active semi-crystalline polyethylenes have been prepared via anionic polymerization of polybutadiene, end-capped with either di-hydroxyl or tetra-hydroxyl functional groups followed by catalytic deuteration. SEC and NMR analysis confirmed that excellent control of molecular weight distribution, functionalization and saturation of the materials was possible, and thermal analysis of the resulting polyethylenes showed that the melting temperatures and apparent fractional crystallinity was virtually independent of functionality of molecular weight. The polymer chain dynamics in the solid state were explored with quasi-elastic neutron scattering, which also showed

that functionalization had very little impact on the chain dynamics. By far the largest single factor affecting the thermal analysis behavior and the solid state dynamics was variation crystallinity, which is governed by fraction of pendant ethyl groups in the chain microstructure.

SANS in the melt state showed that the dihydroxyl functionalized polyethylenes did not form large aggregates or small micelles. There was some evidence of coupling of functional polymers to form dimers, suggesting that the polar functional groups are weakly attracted to each other in the melt. The lack of aggregation is desirable for their utility as blend additives, since aggregation is known to hinder the diffusion and equilibration of functional polymers at interfaces.

In all cases, the functionalized polymers were found to segregate strongly to the silicon-oxide interfaces of blended films at room temperature after annealing above the melting temperature. Interestingly, there was no increase in interfacial activity when the number of hydroxyl groups per chain end on the functional polymer was increased from two to four, and at higher concentrations increasing the size of the functional group decreased its interfacial activity. We speculate that the tetra-hydroxyl functionalized polyethylenes do undergo some aggregation, which in turn limits their ability to diffuse to or adsorb at polar interfaces. For both series of functionalized polyethylenes, there was a broad maximum in interfacial activity as measured by surface excess at 10-15 kg/mol. At low molecular weights, this trend can be explained by the fact that the contribution to the surface excess is proportional to the volume of the adsorbing chain, whereas at high concentrations, the efficiency of adsorption is expected to decrease as the molecular weight of the adsorbing chain approaches that of the matrix polymer.

Finally, we observed a small excess of hydroxyl functionalized PE at the film surface in addition to the accumulation at the buried interface, particularly for lower molecular weight functional PEs. Although the surface excess was insufficient to have a measureable effect on surface hydrophilicity, it could be useful for further functionalization of the PE surface. The reason for the surface excess is not entirely certain, but it appears most likely that it is driven by a combination of the relatively low

molecular weight of the functionalized polyethylene, coupled to the small reduction in surface energy that may be attributable to deuteration.

REFERENCES

(1) Read, D. J.; Auhl, D.; Das, C.; den Doelder, J.; Kapnistos, M.; Vittorias, I.; McLeish, T. C. B. *Science* **2011**, *333*, 1871.

(2) Owen, M. J. In *Physical Properties of Polymers Handbook*; Mark, J. E., Ed.; American Institute of Physics: Woodbury, New York, 1996, p 669.

(3) Holmesfarley, S. R.; Bain, C. D.; Whitesides, G. M. *Langmuir* **1988**, *4*, 921.

(4) Chan, C. M.; Ko, T. M.; Hiraoka, H. *Surface Science Reports* **1996**, *24*, 3.

(5) Woodward, I.; Schofield, W. C. E.; Roucoules, V.; Badyal, J. P. S. *Langmuir* **2003**, *19*, 3432.

(6) Goddard, J. M.; Hotchkiss, J. H. *Progress in Polymer Science* **2007**, *32*, 698.

(7) Ansari, I. A.; Clarke, N.; Hutchings, L. R.; Pillay-Narrainen, A.; Terry, A. E.; Thompson, R. L.; Webster, J. R. P. *Langmuir* **2007**, *23*, 4405.

(8) Hutchings, L. R.; Narrainen, A. P.; Eggleston, S. M.; Clarke, N.; Thompson, R. L. *Polymer* **2006**, *47*, 8116.

(9) Hutchings, L. R.; Narrainen, A. P.; Thompson, R. L.; Clarke, N.; Ansari, I. *Polymer International* **2008**, *57*, 163.

(10) Narrainen, A. P.; Hutchings, L. R.; Ansari, I.; Thompson, R. L.; Clarke, N. *Macromolecules* **2007**, *40*, 1969.

(11) Narrainen, A. P.; Hutchings, L. R.; Ansari, I. A.; Clarke, N.; Thompson, R. L. *Soft Matter* **2006**, *2*, 126.

(12) Thompson, R. L.; Hardman, S. J.; Hutchings, L. R.; Narrainen, A. P.; Dalgliesh, R. M. *Langmuir* **2009**, *25*, 3184.

(13) Narrainen, A. P.; Clarke, N.; Eggleston, S. M.; Hutchings, L. R.; Thompson, R. L. *Soft Matter* **2006**, *2*, 981.

(14) Hardman, S. J.; Muhamad-Sarih, N.; Riggs, H. J.; Thompson, R. L.; Rigby, J.; Bergius, W. N. A.; Hutchings, L. R. *Macromolecules* **2011**, *44*, 6461.

(15) Kimani, S. M.; Hardman, S. J.; Hutchings, L. R.; Clarke, N.; Thompson, R. L. *Soft Matter* **2012**, *8*, 3487.

(16) Bergius, W. N. A.; Hutchings, L. R.; Sarih, N. M.; Thompson, R. L.; Jeschke, M.; Fisher, R. *Polymer Chemistry* **2013**, *4*, 2815.

(17) Clarke, C. J.; Jones, R. A. L.; Edwards, J. L.; Shull, K. R.; Penfold, J. *Macromolecules* **1995**, *28*, 2042.

(18) Hopkinson, I.; Kiff, F. T.; Richards, R. W.; Bucknall, D. G.; Clough, A. S. *Polymer* **1997**, *38*, 87.

(19) Elman, J. F.; Johs, B. D.; Long, T. E.; Koberstein, J. T. *Macromolecules* **1994**, *27*, 5341.

(20) Walters, K. B.; Schwark, D. W.; Hirt, D. E. *Langmuir* **2003**, *19*, 5851.

(21) Hardman, S. J.; Hutchings, L. R.; Clarke, N.; Kimani, S. M.; Mears, L. L. E.; Smith, E. F.; Webster, J. R. P.; Thompson, R. L. *Langmuir* **2012**, *28*, 5125.

(22) Zhu, S. Q.; Hirt, D. E. *Journal of Vinyl & Additive Technology* **2007**, *13*, 57.

(23) Hariharan, A.; Kumar, S. K.; Russell, T. P. *Journal of Chemical Physics* **1993**, *98*, 4163.

(24) Crist, B.; Graessley, W. W.; Wignall, G. D. *Polymer* **1982**, *23*, 1561.

(25) Tanchawanich, J.; Arrighi, V.; Sacchi, M. C.; Telling, M. T. F.; Triolo, A. *Macromolecules* **2008**, *41*, 1560.

(26) Sakai, V. G.; Chen, C. X.; Maranas, J. K.; Chowdhuri, Z. *Macromolecules* **2004**, *37*, 9975.

(27) Arrighi, V.; Tanchawanich, J.; Telling, M. T. F. *Macromolecules* **2013**, *46*, 216.

(28) Sakai, V. G.; Arbe, A. *Current Opinion in Colloid & Interface Science* **2009**, *14*, 381.

(29) *Dynamics of Soft Matter*; Sakai, V. G.; Alba-Simionesco, C.; Chen, S.-H., Eds.; Springer: New York, 2012.

(30) Payne, R. S.; Clough, A. S.; Murphy, P.; Mills, P. J. *Nuclear Instruments & Methods in Physics Research Section B- Beam Interactions with Materials and Atoms* **1989**, *42*, 130.

(31) Thompson, R. L. In *Polymer Science: A Comprehensive Reference*; Moeller, M., Matyjaszwewski, K., Eds.; Elsevier BV: Amsterdam, 2012; Vol. 2, p 661.

(32) Composto, R. J.; Walters, R. M.; Genzer, J. *Materials Science and Engineering R* **2002**, *R38*, 107.

(33) Howells, W. S.; Garcia Sakai, V.; Demmel, F.; Telling, M. T. F. *RAL-TR-2010-006* **2010**.

(34) Azuah, R. T.; Kneller, L. R.; Qiu, Y.; Tregenna-Piggot, P. L. W.; Brown, C. M.; Copley, J. R. D.; Dimeo, R. M. *J. Res. Natl. Inst. Stan. Technol.* **2009**, *114*, 341.

(35) deGennes, P. G. *Scaling Concepts in Polymer Physics*; Cornell University Press: Ithaca, New York, 1979.

(36) Morse, A. J.; Edmondson, S.; Dupin, D.; Armes, S. P.; Zhang, Z.; Leggett, G. J.; Thompson, R. L.; Lewis, A. L. *Soft Matter* **2010**, *6*, 1571.

(37) Barradas, N. P.; Jeynes, C.; Webb, R. P. *Applied Physics Letters* **1997**, *71*, 291.

(38) C.M., H. *Hansen Solubility Parameters: A User's Handbook*; 2nd ed.; CRC Press: Boca Raton, Florida, 2007.

(39) *Polymer Handbook*; 4th ed.; Brandrup, J.; Immergut, E. H.; Grulke, E. A., Eds.; Wiley: New York, 1999.

(40) Arialdi, G.; Karatasos, K.; Rychaert, J. P.; Arrighi, V.; Saggio, F.; Triolo, A.; Desmedt, A.; Pieper, J.; Lechner, R. E. *Macromolecules* **2003**, *36*, 8864.

(41) Arbe, A.; Colmenero, J.; Alvarez, F.; Monkenbusch, M.; Richter, D.; Farago, B.; Frick, B. *Physical Review Letters* **2002**, *89*.

(42) Arbe, A.; Colmenero, J.; Alvarez, F.; Monkenbusch, M.; Richter, D.; Farago, B.; Frick, B. *Physical Review E* **2003**, *67*.

(43) Nicholson, J. C.; Crist, B. *Macromolecules* **1989**, *22*, 1704.

(44) Balsara, N. P. In *Physical Properties of Polymers Handbook*; Mark, J. E., Ed.; American Institute of Physics: Woodbury, New York, 1996, p 257.

(45) Hutchings, L. R.; Richards, R. W. *Macromolecules* **1999**, *32*, 880.

(46) Jones, R. A. L.; Norton, L. J.; Kramer, E. J.; Bates, F. S.; Wiltzius, P. *Physical Review Letters* **1991**, *66*, 1326.

(47) Geoghegan, M.; Jones, R. A. L.; Clough, A. S. *Journal of Chemical Physics* **1995**, *103*, 2719.

(48) Henn, G.; Bucknall, D. G.; Stamm, M.; Vanhoorne, P.; Jerome, R. *Macromolecules* **1996**, *29*, 4305.

(49) Shull, K. R. *Journal of Chemical Physics* **1991**, *94*, 5723.

ACKNOWLEDGMENT. We thank EPSRC for support of this work through EP/G032874/1 and STFC (UK) for provision and support of the neutron facilities at ISIS. We are grateful to Dr Mark Hodgson (DuPont Teijin Films), Mr Peter Reineck (Reineck Associates), Dr JunJie Wu and Prof. Tony Unsworth (Durham University) for many helpful discussions.

Supporting Information Available. S.I.1 Further details of synthesis of multi-end functional polyethylenes; S.I.2. Thermal gravimetric analysis of polymers; S.I.3. AFM height map of film surface; S.I.4.; Influence of N_{agg} on calculated $d\Sigma/d\Omega$ values; S.I.5. Detailed analysis of QENS data for PE materials; S.I.6. Simulated effect of χ_{HD} on $d\Sigma/d\Omega$; S.I.7. Simulated molecular weight dependence of surface excess by SCFT.

SYNOPSIS TOC

Table of Content Image

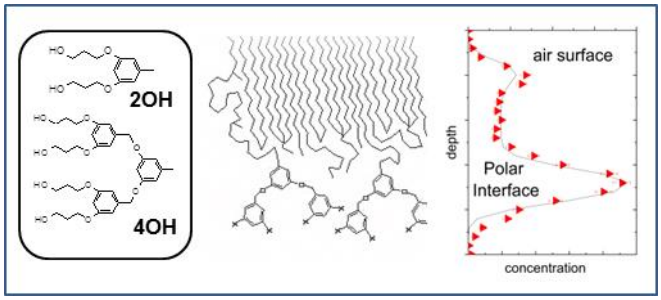

Controlled multiple hydroxyl functionalization of PE yields interfacially active additives with PE-like bulk properties.

SUPPORTING INFORMATION

Supporting Information Available. S.I.1 Further details of synthesis of multi-end functional polyethylenes; S.I.2. Thermal gravimetric analysis of polymers; S.I.3. AFM height map of film surface; S.I.4.; Influence of N_{agg} on calculated $d\Sigma/d\Omega$ values; S.I.5. Detailed analysis of QENS data for PE materials; S.I.6. Simulated effect of χ_{HD} on $d\Sigma/d\Omega$; S.I.7. Simulated molecular weight dependence of surface excess by SCFT.

Supporting Information 1.

Further details of the synthesis of multi-hydroxyl end functional polyethylenes.

Typical syntheses of protected dihydroxy end capping agent (2OX) and tetrahydroxyl end capping agent (4OX) were carried out as follows:

Synthesis of product 3, c.f. main article, scheme 1.

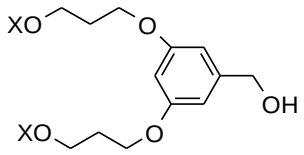

Figure S.I.1. Sketch of product 3.

3,5-dihydroxybenzyl alcohol (1) (26.6 g, 104.9 mmol), 1-bromo-3-(*tert*-butyldimethylsilyoxy) propane (**2**) (7 g, 49.9 mmol), K_2CO_3 (20.7 g, 149.8 mmol) and 18-crown-6 (2.64 g, 10.0 mmol) were added to a round bottomed flask. The solids were then dissolved into dry acetone (300 ml) and the solution was stirred vigorously under reflux for 24 h. At the end of the reaction the pink solution was concentrated by the removal of acetone under vacuum. The product was then extracted using ethyl acetate and water. The organic layer was washed twice with water before drying with $MgSO_4$. The

$MgSO_4$ was removed by filtration and the solvent removed by distillation to yield a yellow oil. The crude product was further purified by column chromatography using silica as the stationary phase and toluene/ethyl acetate (4:1) as the mobile phase. Yield 90.0%, ^{1}H NMR ($CDCl_3$, 400MHz) δ 6.50 (d, 2H, J = 2.2 Hz), 6.34 (t, 1H, J = 2.2 Hz), 4.56 (d, 2H, J = 6.0 Hz), 4.03 (t, 4H, J = 6.0 Hz), 3.78 (t, 4H, J = 6.0 Hz), 1.95 (quintet, 4H, 6 J = 6.0 Hz), 1.69 (t, 1H, J = 6.0 Hz), 0.87 (s, 18H), 0.02 (s, 12H). Element analysis; Calculated $C_{25}H_{48}O_5Si_2$: C, 61.93; H, 9.98. Found: C, 61.90; H, 9.94.

Synthesis of 2OX dendron

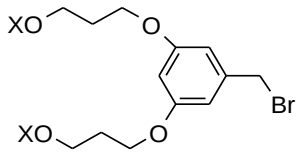

Figure S.I.2. Sketch of product 2OX dendron.

An initial attempt to synthesise 2OX by the Appel reaction using CBr_4/PhP_3 as previously described,[1] was unsuccessful. During the reaction the tert butyldimethylsilyl group which was protecting the alcohol group was cleaved as observed by ^{1}H-NMR therefore an alternative method was used. Into a stirred solution of benzyl alcohol **3** (4.10 g, 8.46 mmol) dissolved into a mixture of dry THF and DCM (10:7), triethylamine (1.65 ml, 11.84 mmol) was added. The flask was then immersed into an ice bath at 0°C. This was followed by the addition of mesylchloride (0.98 ml, 12.69 mmol) and the mixture was stirred for 2 h, after which lithium bromide was added (3.89 g, 44.84 mmol) and mixture allowed to warm to room temperature as it stirred overnight. At the end of the reaction the solvents were removed by distillation and the residue oil was then redissolved in DCM and purified by solvent extraction partioning the oil between water and DCM. The organic layer was then collected and dried over $MgSO_4$. The product (a yellow oil) was then further purified by column chromatography (silica gel as the stationary phase and DCM as the mobile phase) to give a clear oil. Yield 89%, ^{1}HMR ($CDCl_3$ 400 MHz) δ 6.48 (d, 2H, J = 2.2 Hz), 6.34 (t, 1H, J = 2.2 Hz), 4.36 (s, 2H), 3.99 (t, 4H, J = 6.0 Hz), 3.74(t,

4H, J = 6.0 Hz) 1.92(quintet, 4H, J = 6.0 Hz), 0.82 (s, 18H), 0.01 (s, 12H). Element analysis: Calculated $C_{25}H_{47}BrO_4Si_2$: C, 54.82; H, 8.65. Found: C, 54.89; H, 8.64

Synthesis of product 4, c.f. main article, scheme 1

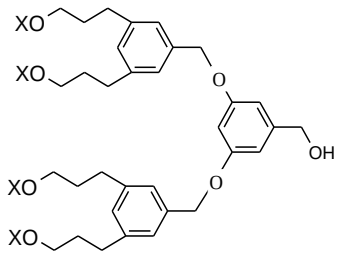

Figure S.I.3. Sketch of product product 4.

Into a round bottomed flask, 3,5-dihydroxybenzyl alcohol (**1**) (0.97 g, 6.96 mmol), **2OX**-dendron (8 g, 15.52 mmol), K_2CO_3 (2.9 g, 22.17 mmol) and 18-crown-6 (0.4 g, 1.48 mmol) were added. The solids were then dissolved into dry acetone (100 ml) and the solution was stirred vigorously under reflux for 24 h. At the end of the reaction the solution was concentrated by removing acetone under reduced pressure and the product extracted using ethyl acetate and water. The organic layer was washed with water before drying with $MgSO_4$. The drying agent was removed by filtration and the filtrate concentrated to yield a yellow oil. The product was further purified by column chromatography using silica as the stationary phase and toluene/ethyl acetate (4:1) as the mobile phase to give product **4**. Yield 92.0%, ^{1}H NMR ($CDCl_3$) δ6.56 (d, 2H, J = 2.1 Hz), 6.51 (d, 4H, J = 2.1 Hz), 6.37 (t, 2H, J = 2.1 Hz), 4.91 (s, 4H), 4.59 (d, 2H, J = 6.0 Hz), 4.00 (t, 8H, J = 6.0 Hz), 3.75 (t, 8H, J = 6.0 Hz), 1.93 (quintet, 8H, J = 6.0 Hz), 1.62 (s, 1H), 0.84 (s, 36H), 0.00 (s, 24H). Element analysis: Calculated $C_{57}H_{100}O_{11}Si_4$: C, 63.76; H, 9.39. Found: C, 63.70; H, 9.36.

Synthesis of 4OX dendron

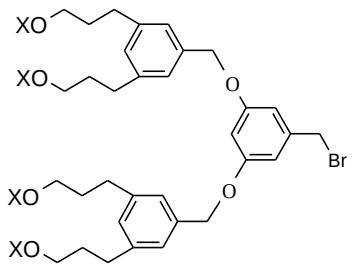

Figure S.I.4. Sketch of product 4OX dendron.

The dendritic benzyl alcohol **4** (8.1 g, 7.55 mmol) was dissolved into a mixture of dry THF and DCM (200ml, 1:1). Into the stirred solution, triethylamine (1.60 ml, 11.17mmol) was added and the flask immersed into an ice bath at 0 °C. This was followed by the addition of mesyl chloride (0.90 ml, 11.32 mmol) and then the mixture was stirred for 2 h, after which lithium bromide was added (3.50 g, 40.02 mmol) and the solution allowed to warm to room temperature as it stirred overnight. At the end of the reaction the solvents were removed under reduced pressure and the residue oil was then redissolved in DCM. The product (a yellow oil) was then further purified by column chromatography (silica gel as the stationary phase and DCM as the mobile phase) to give a clear oil. Yield 85%, ^{1}HMR ($CDCl_3$) δ 6.58 (d, 2H, J = 2.0 Hz), 6.51 (d, 4H, J = 2.0 Hz), 6.37 (t, 2H, J = 2.0 Hz), 4.92 (s, 4H), 4.37 (s, 2H), 4.00 (t, 8H, J = 6.0 Hz), 3.77 (t, 8H, J = 6.0 Hz), 1.93 (quintet, 8H, J = 6.0 Hz), 0.85 (s, 36H), 0.00 (s, 24H). Element analysis: Calculated $C_{25}H_{99}BrO_{10}Si_4$: C, 60.23; H, 8.78. Found: C, 60.30; H, 8.75

A typical synthesis of polyethylene additives, end capped with difunctionalised hydroxyl end capping agent (PE2OH) was carried out as follows: Polyethylene was prepared from polybutadiene using living anionic polymerisation from which the double bonds were saturated, (*c.f.* main text, scheme 2). The same approach was used to synthesise tetrahydroxyl end capped polyethylene (PE4OH). In both cases, a range of additives with different molecular weights were prepared (Table 1).

Living anionic polymerization was carried out using standard high vacuum techniques. For a target molecular weight of 10,000 $gmol^{-1}$, 6.70 g 1,3-butadiene was used, with *sec*-butyllithium (0.48 ml, 1.4 M solution in cyclohexane) as the initiator. The reaction was carried out in hexane (70 ml) at room temperature for 24 h. At the end of the reaction period, hexane and any traces of unreacted monomer were distilled out of the reaction flask and replenished with fresh dry hexane. Into a separate flask that contained dry hexane (5 ml), diphenylethylene, DPE, (0.24 ml, 1.34 mmol) and tetramethylethylenediamine, TMEDA, (0.50 ml, 3.34 mmol) were added through a rubber septum and the contents further purified by titrating *sec*-BuLi into the solution until a permanent reddish colour of diphenylhexyllithium was observed. The purified DPE/TMEDA solution was then injected into the flask that contained living polymer solution and left stirring for 48 hrs at 50 ^{0}C. After this time a sample was taken and quenched with degassed MeOH for analysis. Meanwhile, in a separate flask, a sample of protected hydroxyl end-capping agent (2OX) (**2a**), (0.52 g, 1.00 mmol) was azeotropically dried with benzene three times before dissolving in about 10 ml of dry THF. Into the polymer solution, dry THF (15 ml) was distilled and the solution cooled to -78 °C prior to the addition of a cold solution of the end-capping agent. The reaction was then stirred overnight at -78 °C, during which the red colour of the living polymer dissipated. After this time any unreacted polymer was terminated by addition of nitrogen purged MeOH and the polymer was recovered by precipitation into excess methanol that contained small amount of antioxidant (BHT), dried in *vacuo* to constant mass and stored in the freezer. End-capping with 2OX (**2a**); Molecular weight ($gmol^{-1}$) M_n = 11300, M_w = 11800 (M_w/M_n = 1.04, Figure 1). ^{1}H NMR (700 MHz, CD_2Cl_2, δ, ppm) 5.6 (=CH), 5.4 (=CH), 5.0 (=CH_2 vinyl), 2.2-1.8 (CH_2, polymer backbone), 3.70 (8H, OCH_2CH_2, $ArOCH_2$) OR [C_6D_6 δ, 3.80 (4H, $ArOCH_2$), 3.70 (4H, OTBDMS)], 3.35 (CH_2DPE), 5.7 (2H, ArH), 6.2 (1H, ArH), 7.35-7.15 (Ar-DPE). End-capping with 4OX (**2b**); ^{1}H NMR (700 MHz, CD_2Cl_2, *δ*, ppm): 5.6 (=CH), 5.4 (=CH), 5.0 (=CH_2, vinyl), , 2.2-1.8 (CH_2, polymer backbone), 0.88 (36H, TBDMS), 0.04 (24H, TBDMS), 3.3 (CH_2DPE), 3.79 (8H, OTBDMS), 4.03 ($ArOCH_2$), 4.60 ($ArOCH_2Ar$), 5.7 (2H, ArH), 6.4 (4H, ArH), 6.51 (1H, ArH), 6.6 (2H, ArH), 7.00-7.20 (Ar-DPE).

Deprotection of the alcohol functionality on the product was achieved by acid hydrolysis. This was accomplished using 10 M HCl (10:1 molar ratio with respect to the polymer) under vacuum at 80 °C for 24 h in presence of BHT (1% w/w). The polymer was recovered by precipitation into methanol and dried in a vacuum oven to a constant mass. The hydroxyl functionalised polybutadiene was then saturated to yield linear low density polyethylene, in a 600 ml autoclave at 500 p.s.i. of either hydrogen or deuterium and at 100°C in cyclohexane (1% w/v polymer) using palladium on calcium carbonate (5% by weight Pd; 5-10 m^2 g^{-1} active surface area, catalyst loading was about 2 times the weight of the polymer) for 48 h (deuteration) and 24 h (hydrogenation). The solution was hot filled and the product recovered by precipitation in methanol followed by vacuum drying to a constant mass. In all cases the yields were greater than 90%.

Supporting Information 2.

Thermal Gravimetric Analysis of Polymers

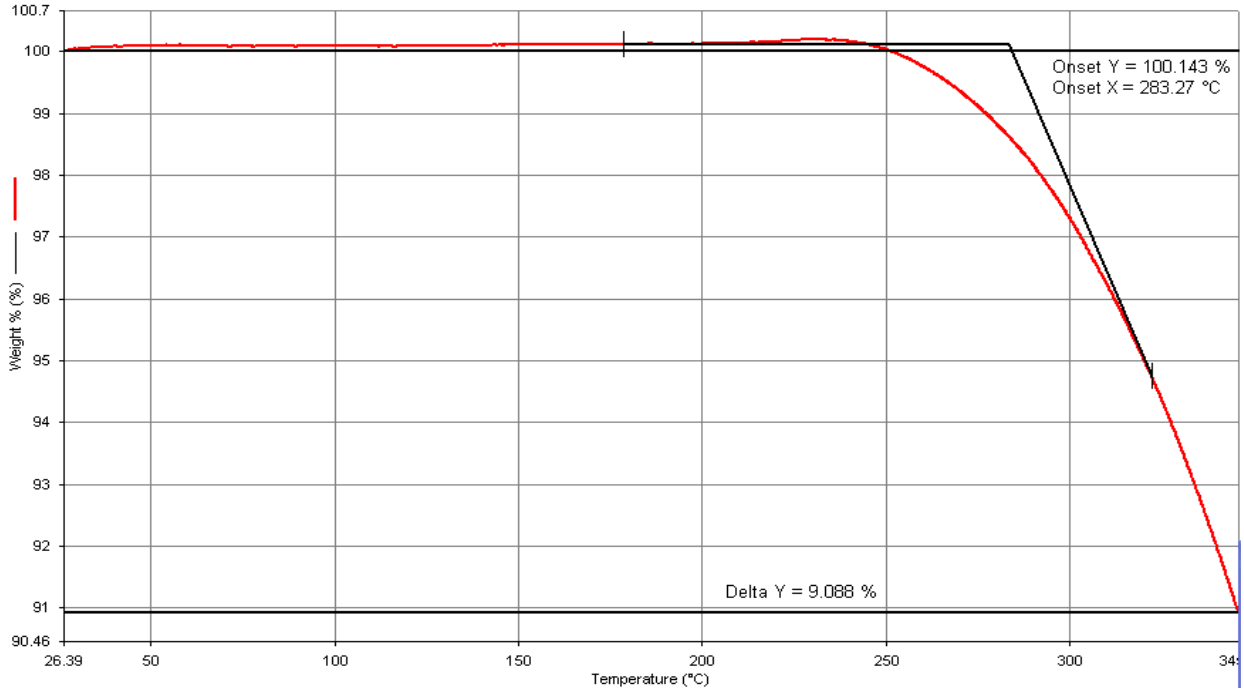

Figure S.I.5. TGA data for 4OHdPE18

Supporting Information 3.

AFM height map of film surface

5μm × 5 μm AFM height map showing crystalline nature of PE blend film. Image obtained using a Bruker MM8 Multimode AFM in ScanAsyst Mode. The vertical range is 30 nm

.

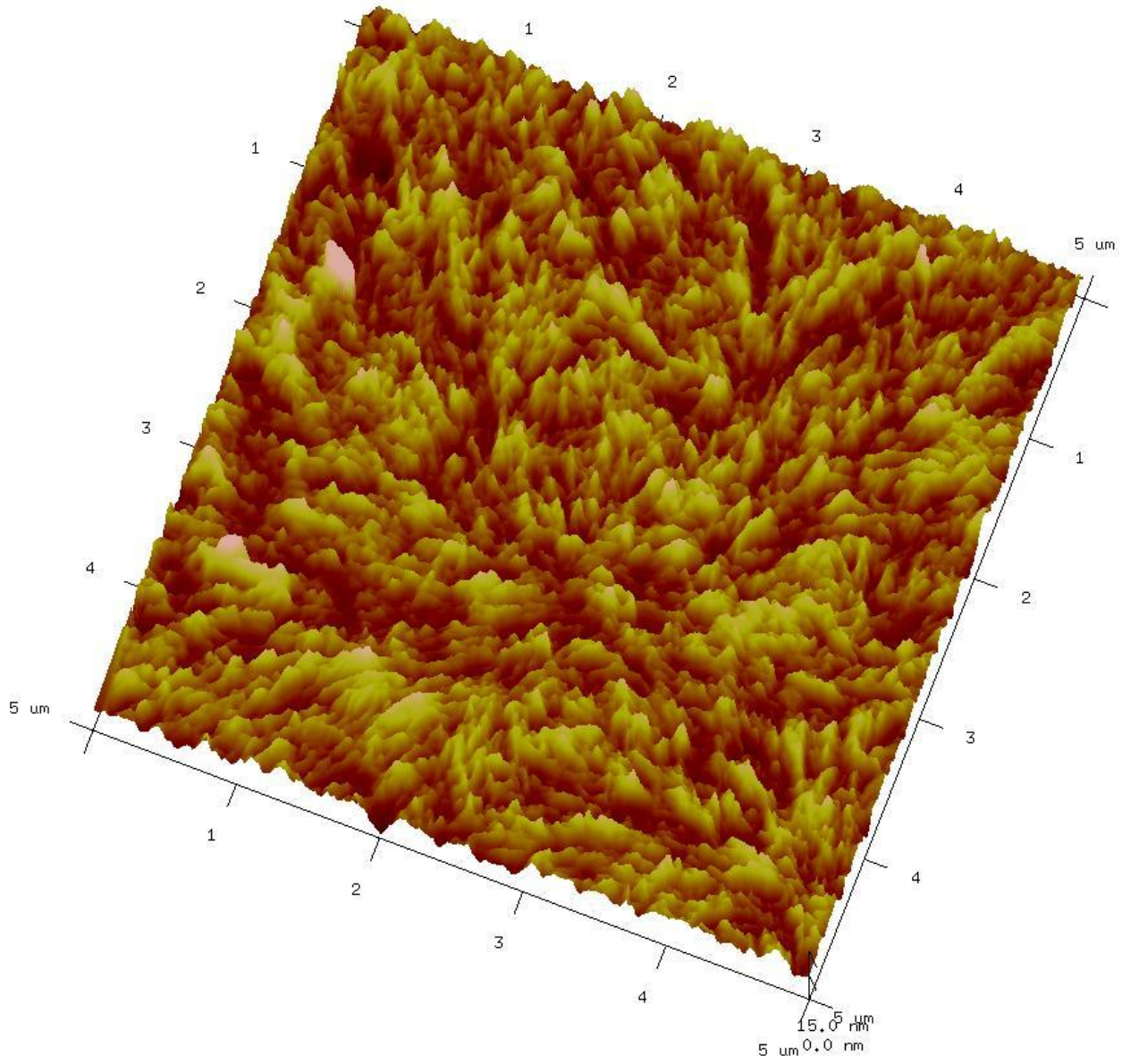

Figure S.I.6. Height map of 12% 2OHdPE22 in hPE blend.

Supporting Information 4
Influence of N_{agg} on calculated dΣ/dΩ values

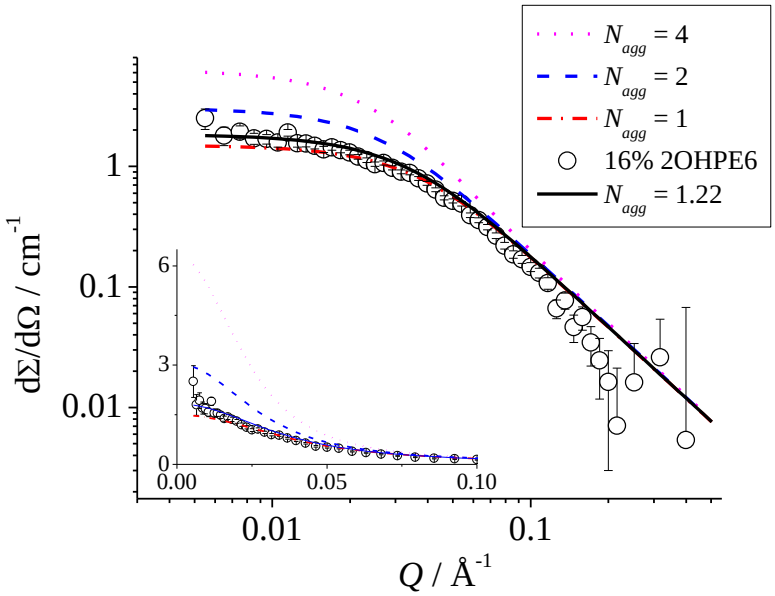

Figure S.I.7. Double log plot of absolute differential scattering cross section data for 16% 2OHdPE6 in hPE. The dotted curves correspond to RPA simulations for unimers, dimers and tetramers of the end functional polymer. The solid curve corresponds to the best fit to the data with an average aggregation number of 1.22. The inset shows the same data and simulations on linear axes.

Supporting Information 5.

Detailed analysis of QENS data for PE materials.

Attempts to fit all of the data with β (from equation 1) fixed at 0.5 would have yielded a dimensionally correct value for a single diffusion coefficient. However, this was not generally successful, and this observation is in accordance with earlier QENS studies on polyethylenes. Arrighi et al[2] studied oligomeric PE at significantly higher temperatures (177 °C) than in our work, and found that *I(Q,t)* was only well fit with $\beta = 0.5$ at $Q < 1$ Å^{-1}, where the diffusive processes would be dominant. Since we found no clear dependence of β on temperature or functionalitity, and the variation was quite small, this parameter was fixed at 0.6 and it was found that all of the data could be well fit (as exemplified in the Main Article, figure 5) using equation 1 by adjusting just *A*, *B (=1-A)* and τ. As would be expected, the greater mobility of the protons at higher temperatures results in a more rapid decay in $I(Q,t)$ as a function of time. The Q dependence of the characteristic relaxation time, τ, is compared in figure S.I.6a for several different PEs at 100 °C. The similarity of the τ values for polymers of similar microstructure, is consistent with the observed similarity in the raw S(Q,E) data in figure 1, but remarkably similar values for τ were also found for the hPE20:80 sample. This indicates that the motions probed by QENS are similar, even for molten hPE20:80 and the other PEs, which are semicrystalline at this temperature. Only at the highest Q values, i.e. shortest length scales, does the relaxation of the molten sample appear to be marginally faster than that of the other polyethylenes. We attribute this to the greater proportion fully hydrogenated of ethyl branches in this sample, which may have enhanced motion over short length scales when compared to protons on the polymer backbone. (The other materials have a smaller proportion of ethyl branches and in the case of the two *x*OHdPE11 materials, the ethyl branches are partially deuterated, so contribute less to the incoherent scattering cross section.)

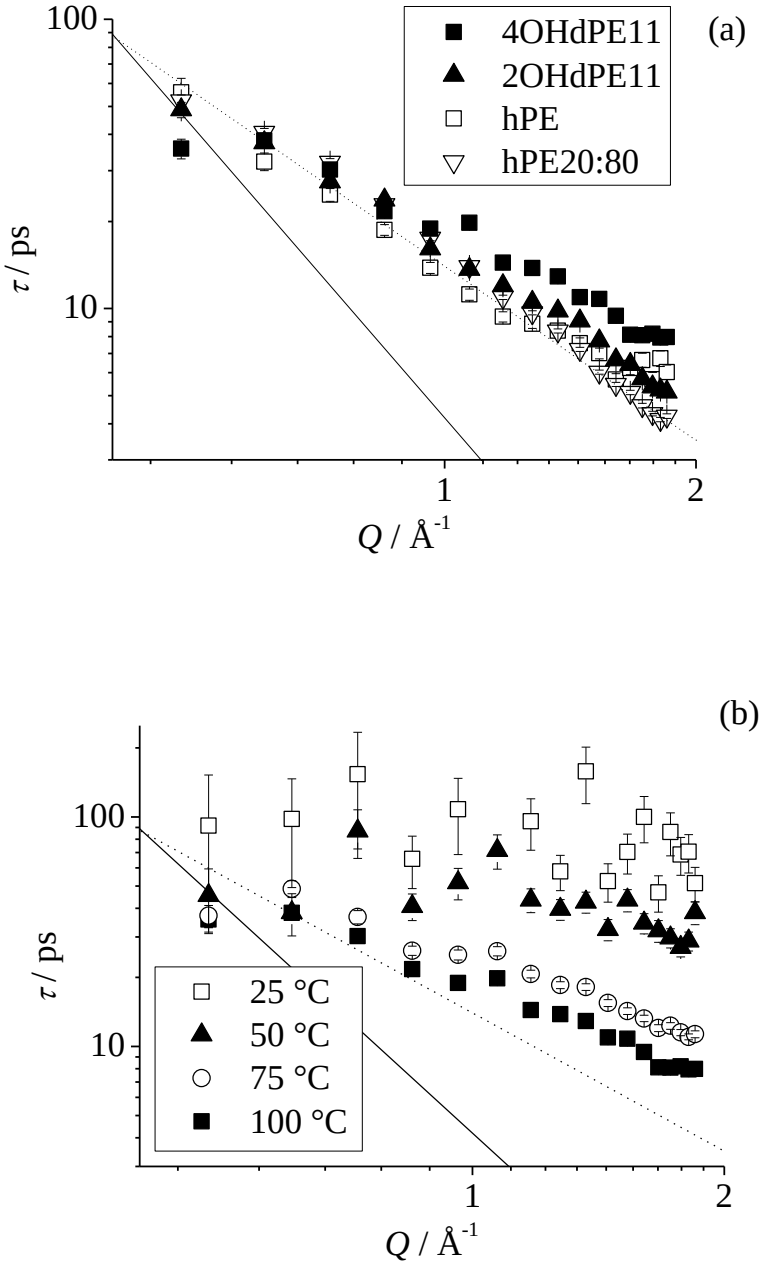

Figure S.I.8. (a) Characteristic relaxation time for several multi-end functional polymers at 100 °C and (b) temperature dependence of relaxation time for 4OHdPE11. The dotted and solid lines indicate a Q^{-2} and $Q^{-2/\beta}$ dependence of τ respectively.

Our results are consistent with the behavior reported by Arbe *et al* for polyisoprenes[3,4] wherein a Q^{-2} dependence of τ, shown as a dashed line in figure S.I.8 (a and b), is indicative of non-Gaussian (jump diffusion) behavior, as opposed to $Q^{-2/\beta}$ dependence expected for Gaussian behavior. At temperatures

below 100 °C, still larger deviations from Gaussian behavior are observed. The loss of Q-dependence in τ at 25 °C and 50 °C indicates that at the lower temperatures, only localized motion (e.g. rotation, torsion) is probed, whereas at 75 °C and 100 °C, a jump-diffusion mode is triggered.

The unexpected similarity in τ values seen for hPE20:80, which is molten at 100 °C and the other materials which are semi-crystalline solids at this temperature can be explained when we consider the proportion of material that is effectively immobile within the QENS window, B. Figure S.I.9 clearly shows that B is much greater for the higher melting polyethylenes than it is for hPE20:80. The differences between the values for B found in the higher melting PEs, combined with the similar values for τ, suggests that the QENS experiments are sensitive to a difference in the fractional crystallinity of the melt pressed samples that was not observed in the DSC experiment (table 1) where the thermal history was more precisely controlled. The Q-dependence of B for the two partially deuterated xOHdPE11 samples is extremely consistent, which further confirms that when the only distintion between the polymers is the size of the end-functional group, the dynamics are virtually unaffected. Despite having the same chain microstructure as the partially deuterated xOHdPE11 materials, the hPE sample has a slightly slower Q dependence and less pronounced the Bragg peak at $Q \sim 1.55$ Å^{-1}. These differences are likely to arise from fully hydrogenated, and relatively mobile, ethyl branches in the chain structure that are unique to the hPE sample; giving this polymer a relatively high incoherent cross section and somewhat lower coherent cross section.

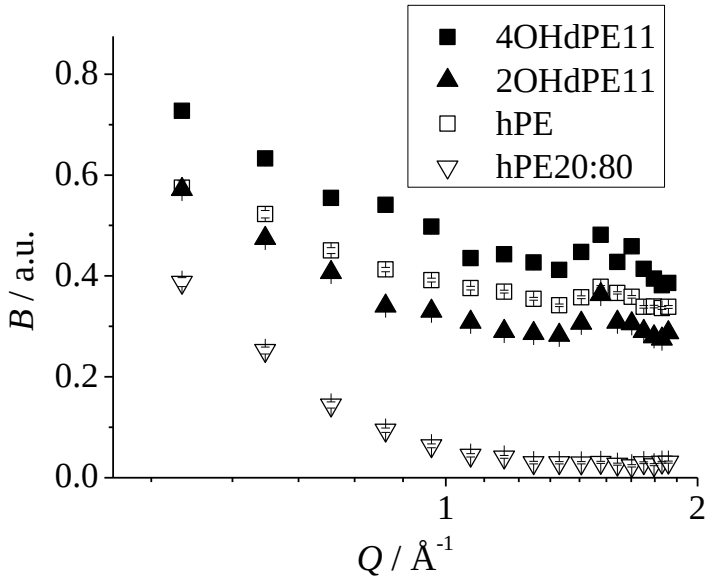

Figure S.I.9. Fitted values for B as a function of scattering vector at 100 °C. Note that the small peak in some data near Q = 1.55 Å^{-1} is an artifact due to the Bragg peak in the elastic scattering, which is seen for all of the semi-crystalline samples.

Supporting Information 6.

Simulated effect of χ_{HD} on dΣ/dΩ;

RPA simulation of influence of Flory Huggins Interaction parameter on absolute differential scattering cross section for the highest molecular weight combination of polymers studied.

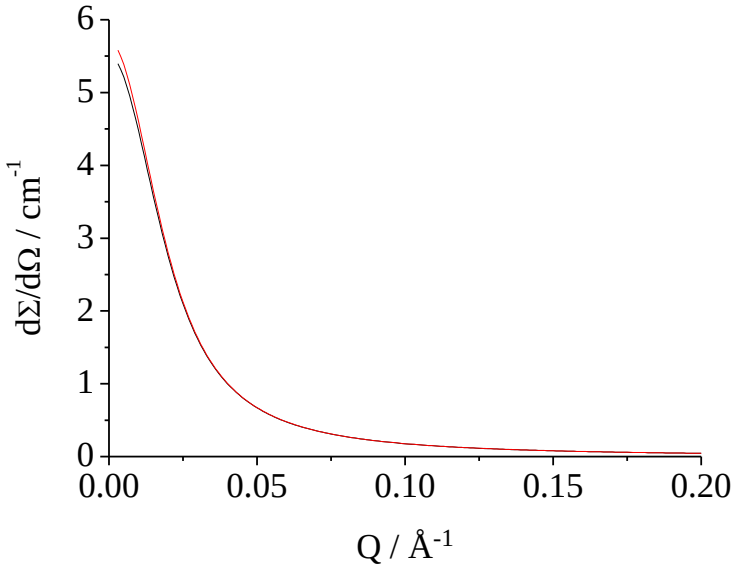

Figure S.I.10. Variation in absolute differential scattering cross section for 2OHdPE22/hPE with interaction parameter, χ, set to 0 (black) and 0.002 (red).

Supporting Information 7.

Simulated molecular weight dependence of surface excess by SCFT

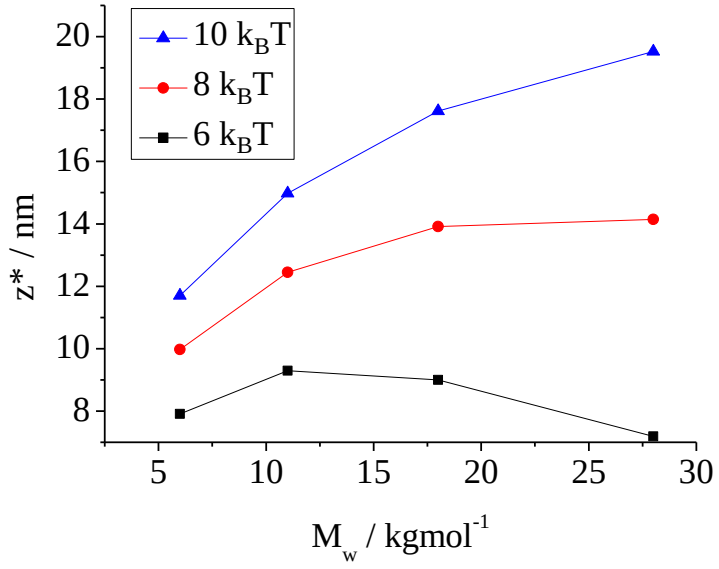

Figure S.I.11. SCFT simulated variation in interfacial excess as a function of adsorbing polymer molecular weight. The volume fraction of adsorbing polymer was fixed at 0.16.

REFERENCES

(1) Kimani, S. M.; Hardman, S. J.; Hutchings, L. R.; Clarke, N.; Thompson, R. L. *Soft Matter* **2012**, *8*, 3487.

(2) Arialdi, G.; Karatasos, K.; Rychaert, J. P.; Arrighi, V.; Saggio, F.; Triolo, A.; Desmedt, A.; Pieper, J.; Lechner, R. E. *Macromolecules* **2003**, *36*, 8864.

(3) Arbe, A.; Colmenero, J.; Alvarez, F.; Monkenbusch, M.; Richter, D.; Farago, B.; Frick, B. *Physical Review Letters* **2002**, *89*.

(4) Arbe, A.; Colmenero, J.; Alvarez, F.; Monkenbusch, M.; Richter, D.; Farago, B.; Frick, B. *Physical Review E* **2003**, *67*.